iTRAQ-based comparative proteomic analysis in mature leaves of Ethiopian mustard (Brassica carinata) provides insights into the whole-proteomic profiles and the role of anthocyanin biosynthesis in leaf color diversity

Tianya Wang
Guizhou University
Shaomin Guo
Guizhou Academy of Agricultural Science
Kunjiang Yu
Guihzou University
Jun Zou
Huazhong Agriculture University
Yingfen Jiang
Anhui Academy of Agricultural Sciences
Wei Wan
Guizhou University
Botao Ye
Guizhou University
Renqin Yang
Guizhou University
Aimal Nawaz Khattak
Guizhou University
Jinling Meng
Huazhong Agriculture University
Entang Tian (erictian121@163.com)
Guizhou University https://orcid.org/0000-0002-9039-3666

Research article

Keywords: Brassica carinata, anthocyanin, iTRAQ, proteomic analysis, purple leaves

Posted Date: September 12th, 2019

DOI: https://doi.org/10.21203/rs.2.14299/v1

Abstract

Background Anthocyanins are the main pigments in leaves, flowers and fruits, performing diverse biological functions in plants and exhibiting benefits for human health. The purple-leaved accession of B. carinata was used to study the biosynthetic mechanism of anthocyanins in this study. To elucidate the mechanisms of anthocyanin accumulation in the purple-leaved line, we employed a proteomic approach based on an isobaric tags for relative and absolute quantification (iTRAQ)-based technique to investigate the protein expression profile of the purple-leaved line of B. carinata in comparison with that of the green-leaved line.

Results In total, 4,631 proteins were identified, of which 285 exhibited significant changes in abundance between BC-G01 and BC-P01. Of the 285 DEPs, 175 are upregulated and 110 are downregulated in the leaves of the purple-leaved line compared with the leaves of the green-leaved line. Bioinformatics analysis indicated that anthocyanin biosynthesis was the most significantly elevated metabolic process, containing three DEPs corresponding to two genes UGT75C1 and UGT79B1 . UGT75C1 and UGT79B1 , encoding anthocyanin 3-O-glucoside: 2”-O-xylosyltransferase and anthocyanin 5-O-glucosyltransferase, respectively, play an important role in the biosynthesis of anthocyanins.

Conclusions The exact functions of these proteins remain to be examined. Nevertheless, our study paves the way for understanding the genetic regulatory mechanisms of anthocyanin biosynthesis and accumulation in B. carinata .

Background

Brassica carinata (BBCC, 2n = 34) is an important vegetable and oilseed crop in northeast Africa and is thought to have originated in the Ethiopian plateau [1–3]. Together with another two amphidiploid *Brassica* species, namely, *B. napus* (AACC, 2n = 38) and *B. juncea* (AABB, 2n = 36), in the U-triangle, *B. carinata* is an amphidiploid of recent origin [2, 4, 5]. Cytogenetic and molecular evidence suggests that *B. carinata* has evolved as a natural cross between *B. oleracea* (CC, 2n = 18) and *B. nigra* (BB, 2n = 16), followed by subsequent chromosome doubling [5–8]. The lengthy processes of speciation and domestication have resulted in diverse eco-types with the whole range of morphological and agronomic differences [8–10]. Given the many desirable characteristics of *B. carinata,* such as resistance to pests, tolerance to diseases and drought, and applicability as a bio-industrial oil crop [11, 12], we made great efforts to study and utilize the species, such as by transferring the yellow-seeded trait to *B. napus* from *B. carinata* [13], evaluating the genetic diversity of 110 accessions of *B. carinata* with emphasis on the interspecific crossability with *B. rapa* [10], synthesizing the *Brassica* trigenomic allohexaploid via *B. carinata×B. rapa* [14], generating the new-type *B. napus* by incorporating components of the C genome of *B. carinata* into traditional *B. napus [*15, 16], assessing the genetic introgression from *B. carinata* into new-type *B. napus* breeding lines [17], construction of one double-haploid mapping population of *B. carinata* and QTL mapping of petal and anther tip color, seed coat color, flower development and quality

traits [2, 18, 19]. As continued research, we attempted to exploit the proteomic profiles and identify the key genes associated with anthocyanin biosynthesis in purple-leaved *B. carinata* in this study.

Anthocyanins are the main pigments in leaves, flowers and fruits and are responsible for the red-to-blue colors of plant organs [20, 21]. Approximately 17 anthocyanidins are found in nature, but only 6 are widely distributed: cyanidin, delphinidin, petunidin, peonidin, pelargonidin, and malvidin [21, 22]. The individual anthocyanidin content varies among species with respect to the following features: (i) the number and positions of hydroxyl (OH) groups, (ii) the degree of methylation of these OH groups, (iii) the nature, number, and location of sugars attached to the molecule, and (iv) the nature and number of aliphatic or aromatic acids attached to the sugar [21, 23]. In addition, the colorful appearance of different organs depends on the pH value of the anthocyanin solution, because of the ionic nature of the molecular structure of anthocyanins [24, 25]. In the present study, the leaves of *B. carinata* appear purple; anthocyanins have a purple hue in neutral pH, but the color changes to blue with increasing pH [25]. Natural mutants with purple organs have been found and reported in many species, such as in asparagus [26], crackers and bars of wheat [27], rice [28], eggplant [29], corn [30], carrot, potatoes [31], basil [32], tea [33], and pepper [34] and in the *Brassica* U-triangle species *B. oleracea* [35], *B. napus* [36], *B. rapa* [37], and *B. juncea* [38], in addition to *B. nigra* and *B. carinata.* The purple color resulting from the presence of anthocyanins in different species can be used as a natural food colorant, and these compounds have health-associated nutraceutical properties.

iTRAQ is a novel, MS-based approach for the relative quantification of proteins, relying on the derivatization of primary amino groups in intact proteins using an isobaric tag for relative and absolute quantitation [39]. This method has been widely used in the identification of key proteins related to target traits in recent years. In the present study, the high-throughput iTRAQ methodology was used to investigate protein and qualitative changes between the two double-haploid lines of *B. carinata* with purple and green leaves. To the best of our knowledge, this is the first report of proteomic research related to purple leaves in *B. carinata.* This study provides novel insights into the proteomic profile of *B. carinata* and for identification of the key protein involved in anthocyanin biosynthesis in this species.

Methods

Plant materials

Two *B. carinata* double-haploid (DH) lines, namely, BC-P01 and BC-G02, were used in this study. BC-P01 and BC-G02, originally named CGN03981 and CGN03976, respectively, were obtained from the Centre for Genetic Resources, Wageningen, the Netherlands (CGN, http://www.cgn.wur.nl/NL/) [10]. In October 2017, BC-P01 and BC-G02 were planted at the farm of Guizhou University, Guiyang, China. In December 2018, three randomly selected plants for each of BC-P01 and BC-G02 were chosen for picking of leaf samples. The fifth mature leaf from the ground for each plant was sampled and transferred into a −80°C freezer for storage.

Determination of total anthocyanin content

The total anthocyanin content was estimated by the simplified method and pH differential method, respectively. For the pH differential method, six freeze-dried leaf samples (0.5 g) were ground to a powder and then extracted twice with 25 ml of methanol:water:acetic acid (V:V:V = 85:15:0.5) at 50 ℃ for 2 h. The extract solution was collected and filtered through a 0.22 μm filter to measure the absorbance according to Wang et al. [40] and Zhao et al. [38]. Determination of the absorbance of the extracts was performed with a SPECORD 200 PLUS UV spectrophotometer (Analytik Jena AG, Jena, CA). In our experiment, the optimum temperature was 50℃, and the equilibration times for pH 1.0 and pH 4.5 were 80 min and 100 min, respectively. The total absorbance (A) was calculated as follows: A = (A510 - A700) pH 1.0 - (A510 - A700) pH 4.5. Then, the total anthocyanin content (TAC) was estimated as C ($mg{\cdot}g^{-1}$) = (A×V×n×M)/(ε×m) [A: the absorbance difference between pH 1.0 and pH 4.5; V: total volume of extract (mL); n: dilution factor; M: relative molecular mass of cyanidin–3-glucoside (449.4); ε: extinction coefficient of cyanidin–3-glucoside (26900); m: sample mass (g)] according to Wang et al. [40] and Cheng et al. [41]. For the simplified method, most steps were performed according to Wang et al. [42] and Yu et al. [43] with minor modifications. Determination of the absorbance of the extracts was performed on a SPECORD 200 PLUS UV spectrophotometer (Analytik Jena AG, Jena, CA). The anthocyanin content is expressed in g·10 ml 0.1 mol/L hydrochloric acid.

Protein extraction for iTRAQ analysis

Total proteins from the sixth samples were extracted according to the following procedure. Approximately 1.0 g of the ground-up leaf powder of each sample was combined with 4 ml of 10% m/v trichloroacetic acid (TCA) in acetone, and the samples were incubated at −20°C for 2 h. The samples were then centrifuged at 20,000 ×g for 30 min at 4°C. The supernatant was discarded without disturbing the pellets. To reduce acidity, the pellets were washed with acetone and incubated at −20°C for 30 min and centrifuged at 20,000 ×g for 30 min at 4°C. The washing step with acetone was repeated several times until the pellets were white. The dried pellets were lysed with 1 ml of protein extraction reagent [8 M urea, 30 mM HEPES, 1 mM PMSF, 2 mM EDTA and 10 mM DTT]. The pellets were then dissolved by ultrasonication (pulse on 2 s, pulse off 3 s, power 180 w) for five minutes. After dissolution, the solution was centrifuged at 20,000 ×g for 30 min at 4°C to remove insoluble impurities. Proteins were reduced with 10 mM DTT at 56°C for 1 h and alkylated immediately with 55 mM iodoacetamide (IAM) in the dark at room temperature for 1 h. The treated proteins were precipitated in acetone at −20°C for 3 h. After centrifugation at 20,000 ×g for 30 min at 4°C, the pellets were resuspended and ultrasonicated in prechilled 50% TEAB buffer with 0.1% SDS and dissolved by ultrasonication. The proteins were regained after centrifugation at 20000 ×g for 30 min, and the protein concentration was determined by the Bradford assay (Bio-Rad) using BSA as a standard.

In-solution digestion and iTRAQ labeling

For each sample, 100 µg of protein in TEAB buffer was incubated with 3.3 µg of trypsin (1 µg/µl) (Promega, Madison, WI, USA) at 37°C for 24 h in a sealed tube. The tryptic peptides were lyophilized and dissolved in 50% TEAB buffer. Samples were labeled using the iTRAQ Reagents 8-plex Kit according to the manufacturer's instructions (AB Sciex Inc., MA, USA). A total of 100 µg of protein in TEAB buffer was incubated with 3.3 µg of trypsin (1 µg/µl) (Promega, Madison, WI, USA) at 37°C for 24 h in a sealed tube. The tryptic peptides were lyophilized and dissolved in 50% TEAB buffer. Samples were labeled using the iTRAQ Reagents 8-plex Kit according to the manufacturer's instructions (AB Sciex Inc., MA, USA).

HPLC (strong cation exchange)

The labeled samples were then alkalified and fractionated using a strong cation exchange HPLC system (Agilent 1100, USA) connected to an SCX column (Luna 5u column, 4.6 mm×250 mm, 5 µm, 100 Å; Phenomenex, Torrance, CA). The retained peptides were eluted using Buffer A (10 mM KH_2PO_4 in an aqueous solution of 25% acetonitrile and acidified to a pH of 3.0 with H_3PO_4) and Buffer B, where Buffer B was composed of Buffer A with 2 M KCl. The fractions were collected in 1.5-ml microfuge tubes with a flow rate of 1 ml/min. The following chromatographic gradient was applied: 0~25 min 100% Buffer A; 0~10 min 5% Buffer B; 10~40 min 5–30% Buffer B; 40~45 min 30–60% Buffer B, 45–55 min 60–80% Buffer B; 55–65 min decreasing to 5% Buffer B. Fraction collection was started 26 min after the injection with a sample collected every 1 min to obtain a total of 38 fractions. Eluted fractions were dried in a vacuum concentrator, and each fraction was dissolved in 0.1% formic acid solution prior to reversed-phase nano-LC-tandem mass spectrometry (LC-MS/MS).

LC-MS/MS analysis

The peptides were dissolved with 50 µl of mobile phase A (H_2O, 0.1% formic acid) and loaded onto an Acclaim PePmap C18 reversed-phase column (75 µm×2 cm, 3 µm, 100 Å, Thermo Scientific) and separated with a reversed-phase C18 column (75 µm×10 cm, 5 µm, 300 Å, Agela Technologies) mounted on a Dionex Ultimate 3000 nano-LC system. Peptides were eluted using the following gradient: 0~6 min 5% Buffer B; 6~6.5 min 10% Buffer B; 6.5~45 min 10–24% Buffer B; 45~51 min 24–40% Buffer B, 51–54 min 40–80% Buffer B; 54–59 min 80% Buffer B; 59–59.9 min decreasing to 5% Buffer B; 59.9–65 min 5% Buffer B. The elution was performed at a flow rate of 300 nl min−1, and the instrument was coupled with a Q Exactive mass spectrometer (Thermo Fisher Scientific, MA, USA). The eluates directly entered the Q-Exactive MS instrument (Thermo Fisher Scientific, Waltham, MA, USA), and the experiment was performed in positive-ion mode and in a data-dependent manner with full MS scan from 350–2000 m/z, full scan resolution at 70,000, MS/MS scan resolution at 17,500. MS/MS scan with minimum signal threshold 1E+5, and isolation width at 2 Da. To evaluate the performance of this mass spectrometry experiment with the iTRAQ-labeled samples, two MS/MS acquisition modes and higher-energy collisional dissociation (HCD) were employed. To optimize the MS/MS acquisition efficiency of HCD, normalized collision energy (NCE) was systemically examined from 20% and determined to be optimal at 28% NCE.

Protein identification and quantification

Peptide identification and quantification was carried out on PD（Proteome Discoverer）software, version 1.3 (Thermo), and with the integrated false discovery rate (FDR) analysis function. The data were searched against a protein sequence database downloaded from the BUSCO https://busco.ezlab.org/database. The MS/MS spectra obtained were searched using the following user-defined search parameters: sample type: iTRAQ 8-plex (peptide labeled); cysteine alkylation; digestion: trypsin; instrument: Q-Exactive; species: *Brassica carinata;* search effort: thorough. For the FDR analysis, the MS/MS spectra were searched against a decoy database to estimate the false discovery rate (FDR) for peptide identification. The decoy database consisted of reversed protein sequences from the *Candida albicans* database. The resulting data set was auto-bias-corrected to remove any variations caused by unequal mixing during the combination of different labeled samples. Different modification states of the same peptide sequences are considered distinct by the software.

Results

Phenotypic characterization of BC-P01 and BC-G02

The total anthocyanin content (TAC) of the two double-haploid (DH) lines BC-P01 (purple leaves) and BC-G02 (green leaves) of *B. carinata* were determined by the pH-based color difference method and simplified method (Fig. 1). The leaves of the BC-P01 line were purple from emergence to senescence. The TAC of BC-P01 was 22.7 g·10 mL 0.1 mol/L hydrochloric acid, which was significantly higher than that that of BC-G02 (0.97 g·10 mL 0.1 mol/L hydrochloric acid), as determined by the simplified method ($p = 0.000$) (Fig. 1). In addition, the TAC of BC-P01 22.7 was 3.70 $mg \cdot g^{-1}$, which was significantly higher than that of BC-G02 (0.05 $mg \cdot g^{-1}$), as determined by the simplified method ($p = 0.000$) (Fig. 1).

Protein identification and quantification

In this study, a total of 35,296 matched spectra were identified from mature leaves of *B. carinata* with different colors using the iTRAQ technique (Supplementary Fig. 1A). After eliminating low-scoring spectra, the reset spectra were matched to 1,7307 peptides; a total of 4,631 proteins were identified from Ethiopian mustard, and 3,442 proteins were quantifiable (Supplementary Fig. 1A). In addition, the relative molecular mass of all the identified proteins was more than 10 kDa (Supplementary Fig. 1B). Most of the identified peptides were unique peptides (Supplementary Fig. 1C). The number of amino acids in the peptide sequences was mainly between 7 and 35 (Supplementary Fig. 1D). The sequence coverage of most of the proteins in Ethiopian mustard leaves was higher than 5% (Supplementary Fig. 1E). These results indicated that the proteomics analysis is reliable. In addition, we detected 1,837 transcription factors (TFs), including 160 *bHLH*-type proteins, 136 *MYB*-related proteins, 125 *FAR1*-type proteins, 119 B3-type proteins, and 118 *NAC*-type proteins (Supplementary Fig. 1F).

Through comparisons between purple leaves and green leaves of Ethiopian mustard, a total of 285 differentially expressed proteins (DEPs) were identified from three biological replications with p value<0.05 (Supplementary Table 1). Of the 285 DEPs, 175 are upregulated and 110 are downregulated in the leaves of BC-P01 compared with the leaves of BC-G02. These DEPs between BC-P01 and BC-G01 were revealed by a hierarchical clustering analysis (Supplementary Fig. 2 and Supplementary Table 2).

Functional classification analysis

Gene Ontology (GO) functional annotation analysis was used to further clarify the functional distributions of the 285 DEPs. The results covered a wide range of biological processes, cellular components and molecular functions, which could be classified into 17, 12, and 11 categories, respectively (Fig. 2 and Supplementary Table 3). Some DEPs were assigned to more than one subcategory. In the “biological process” category, the first three classifications included “cellular process” (121 upregulated DEPs (67.98%) and 62 downregulated DEPs (55.86%), “metabolic process” (106 upregulated DEPs (59.55%) and 61 downregulated DEPs (54.95%) and “response to stimulus” (74 upregulated DEPs (41.57%) and 41 downregulated DEPs (36.94%) (Fig. 2 and Supplementary Table 3). In the “cellular component” category, the first three classifications included “cell part” (151 upregulated DEPs (84.83%) and 83 downregulated DEPs (74.77%), “organelle” (107 upregulated DEPs (60.11%) and 63 downregulated DEPs (56.76%) and “organelle part” (63 upregulated DEPs (35.39%) and 43 downregulated DEPs (38.74%) (Fig. 2 and Supplementary Table 2). In the “molecular function” category, the first three classifications included “catalytic activity” (103 upregulated DEPs (57.87%) and 68 downregulated DEPs (61.26%), “binding” (107 upregulated DEPs (60.11%) and 53 downregulated DEPs (47.75%), and “molecular function regulator” (8 upregulated DEPs (4.49%) and 5 downregulated DEPs (4.5%) (Fig. 2 and Supplementary Table 3). These results provided primary proteomic information for DEPs between lines BC-P01 and BC-G02 of *B. carinata.* We also found that the expression of DEPs in BC-P01 with purple leaves was significantly higher than the number of DEPs in BC-G02 with green leaves.

In addition, COG annotation of the DEPs was also performed (Fig. 3 and Supplementary Table 4). All these DEPs were divided into 25 categories, and some DEPs were assigned to more than one subcategory. The first three classifications were “Translation, ribosomal structure and biogenesis” (259 DEPs), “General function prediction only” (223), “Posttranslational modification, protein turnover, chaperones” (196), “Amino acid transport and metabolism” (165), “Carbohydrate transport and metabolism” (159) and “Energy production and conversion” (158). Overall, the expression levels of DEPs in different categories in BC-P01 with purple leaves was significantly higher than that in BC-G02 with green leaves.

The main biochemical metabolism and metabolic pathways associated with the DEPs were also described via KEGG pathway database analysis. The results showed that all the annotated proteins were mapped onto 84 KEGG pathways (Supplementary Table 5). The pathways were mainly related to carbon metabolism (including 7 upregulated proteins and 10 downregulated proteins), biosynthesis of amino

acids (8 upregulated and 2 downregulated proteins), 2-oxocarboxylic acid metabolism (8 upregulated and 0 downregulated proteins), phenylpropanoid biosynthesis (8 upregulated and 0 downregulated proteins), pyruvate metabolism (1 upregulated and 6 downregulated proteins), glutathione metabolism (6 upregulated and 1 downregulated proteins), plant-pathogen interaction (6 upregulated and 1 downregulated proteins), protein processing in endoplasmic reticulum (7 upregulated and 0 downregulated proteins), and so on. Bioinformatics analysis indicated that five metabolic processes, namely, anthocyanin biosynthesis (map00942), carbon metabolism (map01200), 2-oxocarboxylic acid metabolism(map01210), ascorbate and aldarate metabolism (map00053) and tryptophan metabolism (map00380), were the most significantly elevated metabolic processes. Overall, KEGG pathways were identified for 147 upregulated DEPs and 104 downregulated DEPs.

The anthocyanin biosynthesis pathway

The anthocyanin content was synthesized by one complex metabolic pathway. In this study, three upregulated proteins were identified to be involved in one significant metabolic pathway (map00942, Fig. 4 and Table 1). The fold change values for the proteins TRINITY_DN5961_c0_g2, TRINITY_DN5961_c0_g1 and TRINITY_DN8427_c0_g1 were 2.13, 2.07 and 2.32, respectively. These proteins correspond to two anthocyanin 5-O-glucosyltransferases and an anthocyanin 2”-O-xylosyltransferase, and the genes that encode these proteins are *UGT75C1* and *UGT79B1,* respectively.

Discussion

The synthesized plant TACs, including mainly cyanidin, delphinidin, petunidin, peonidin, and pelargonidin, can determine plant organ color at specific pH values, which is why the Ethiopian mustard leaves in this study were purple in color. Three upregulated proteins corresponding to the two genes *UGT75C1* and *UGT79B1* were identified by iTRAQ. The protein expression levels in BC-P01 with purple leaves was more than two times that in BC-G02 with green leaves. These two genes should be the key genes associated with the color difference between lines BC-P01 and BC-G02 of *B. carinata*. *UGT75C1* and *UGT79B1* are involved in the complex metabolic pathways of TAC metabolic synthesis. *UGT79B1* (At5g54060), encoding anthocyanin 3-O-glucoside: 2”-O-xylosyltransferase, together with *At3AT1* and *At3AT2* (At1g03490 and At1g03495), is responsible for the glycosylation and acylation of cyanidin 3-O-glucoside (Cy3G) to produce cyanidin 3-O-[2”-O-(xylosyl)−6”-O-(p-coumaroyl) glucoside] [44–46]. Then, the cyanidin 3-O-[2”-O-(xylosyl)−6”-O-(p-coumaroyl) glucoside] can be glucosylated by UGT75C1 (At4g14090), encoding anthocyanin 5-O-glucosyltransferase, to produce cyanidin 3-O-[2”-O-(xylosyl)−6”-O-(p-coumaroyl) glucoside] 5-O-glucoside [46, 47]. These studies indicate that *UGT75C1* and *UGT79B1* play an important role in TAC synthesis. By utilization of high-throughput RNA sequencing, the expression of *UGT75C1* and *UGT79B1* was found to be positively correlated with TAC biosynthesis [47, 48]. In addition, the expression of *UGT75C1* and *UGT79B1* was found to be significantly high in purple buds and leaves of tea [49] and in light purple petals compared with white petals [50], respectively. These results are consistent with this study because the protein expression level of *UGT75C1* and *UGT79B1* was

upregulated in BC-P01 compared with BC-G02. To date, almost no studies related to *UGT75C1* and *UGT79B1* expression at the protein level have been reported. The proteins identified in this study by iTRAQ can provide useful information for studying the metabolic pathway of TAC synthesis in *B. carinata* and other species in Brassiceae.

The TAC metabolic pathway can be regulated by primary metabolism, including sucrose, starch, and hexose sugars. Sucrose is generally the major end product of photosynthetic carbon metabolism, and in most plants, it is the predominant form of carbon transported to the heterotrophic tissues [51, 52]. The significant metabolic pathway of the carbon metabolism pathway may be the important reason for the color difference between BC-P01 and BC-G02 in this study. Sucrose could provide precursors and sugar moieties for TAC synthesis. In addition, sucrose can specifically induce the TAC biosynthetic pathway for signaling, and these signal transduction pathways may lead to the activation or inactivation of gene expression [20, 53–55]. The degradation of starch can contribute to anthocyanin accumulation in the tuberous root of purple sweet potato [56]. The TAC metabolic pathway can be affected by some other hormones, such as methyl jasmonate [55], GA [57], abscisic acid [58, 59], BPA [60], ethylene [61], and hematin [62]. TAC synthesis can also be regulated by fertilizers [63], such as nitrogen [64, 65] and phosphate [66]. Light [67–70], short-day signals [71] and low temperature [72] can also affect the TAC biosynthesis pathway. Therefore, all of the pathways involved in the synthesis, degradation and absorption of these factors can regulate TAC biosynthesis in this study.

The genetic transcription of genes in the TAC biosynthetic pathway can be regulated by a combination of transcription factors (TFs). The regulatory effects of TFs on TAC biosynthesis have been reported in many studies. The TFs include MYB, bHLH, and WDR. In *Arabidopsis thaliana,* the PAP1-GL3-TTG1 complex can regulate the TFs of MYB and bHLH [73]. In addition, the reduction of MYB expression can reduce the expression levels of *DFR, LDOX, GST12, F3'H* and *UGT75C1* in the TAC pathway [74]. *UGT75C1* is also upregulated by *PAP1,* encoding an MYB transcription factor [47]. As a whole, the TF complex (TT2, TT8, and TTG1) and SmMYB1, an R2R3 MYB transcription factor, can regulate all anthocyanin pathway genes [73, 75]. In this study, we identified thousands of TFs, including TFs for TAC synthesis, which might be involved in the regulation of genes in the TAC metabolic pathway.

Conclusions

In this study, an iTRAQ-based proteomic study was carried out to investigate the protein expression profile of the purple-leaved line of *B. carinata* in comparison with that of the green-leaved line. Identified DEPs by bioinformatics analysis were mainly associated with “translation, ribosomal structure and biogenesis”, “general function prediction only”, “posttranslational modification, protein turnover, chaperones”, “amino acid transport and metabolism”, “carbohydrate transport and metabolism” and “energy production and conversion”. For anthocyanin biosynthesis, three DEPs, corresponding to two genes UGT75C1 and UGT79B1, might play an important role. Our results provide insights into whole-proteomic profiles and regulatory genes that may be responsible for anthocyanin biosynthesis in *B. carinata,* and suggest that

future efforts will be directed towards understanding how these candidate genes regulate the anthocyanin biosynthesis pathways in this species.

Abbreviations

iTRAQ: isobaric tags for relative and absolute quantification; TCA: trichloroacetic acid; IAM: iodoacetamide; HCD: higher-energy collisional dissociation; NCE: normalized collision energy; PD: proteome discoverer; FDR: false discovery rate; TAC: total anthocyanin content; DEPs: differentially expressed proteins; GO: gene ontology; COG: clusters of orthologous group; KEGG: kyoto encyclopedia of genes and genomes; TFs: transcription factors

Declarations

Acknowledgments

Not applicable.

Ethics approval consent to participate

Not applicable.

Authors' contributions

ET conceived and designed the experiments. TW, SG, WW, YB, RY and ANK performed the experiments. TW, SG and ET analyzed the data and wrote the paper. ET, SG, KY, JZ, YJ and JM revised the paper. All authors read and approved the final manuscript.

Funding

The financial of this research was supported by the National Natural Science Foundation of China (grant no. 31560422), Agricultural Science and Technology Support Program of Guizhou Province (Qiankehe Zhicheng no. [2019]2396), Science and Technology Foundation of Guizhou Province of China (grant no. Qiankehe J zi [2015]2052), Scientific Research Foundation for Returned Scholars, Ministry of Education of China (grant no. Jiaowaisiliu [2015]1098), Foundation of Guizhou University (grant no. Guidarenjihezi [2014]14), and Construction Program of Biology First-class Discipline in Guizhou (grant no. GNYL[2017]009).

Availability of data and materials

All data sets generated as part of this study are available at the additional files of this study.

Consent for publication

Not applicable.

Competing interests

The authors declare that they have no competing interests.

Author details

[1]Agricultural College of Guizhou University, Guizhou University, Guiyang 550025, China. [2]Institute of Rapeseed Research, Guizhou Academy of Agricultural Science, Guiyang 550018, China. [3]National Key Laboratory of Crop Genetic Improvement, Huazhong Agricultural University, Wuhan 430070, China. [4]Anhui Academy of Agricultural Science, Hefei 230001, China.

References

1.Warwick SI: *Brassicaceae in Agriculture.* In: *Genetics and Genomics of the Brassicaceae.* Edited by Schmidt R, Bancroft I. New York, NY: Springer New York; 2011: 33–65.

2.Guo S, Zou J, Li R, Long Y, Chen S, Meng J: *A genetic linkage map of Brassica carinata constructed with a doubled haploid population. Theoretical and Applied Genetics* 2012, *125(*6):1113–1124.

3.Warwick SI, Gugel RK, McDonald T, Falk KC: *Genetic Variation of Ethiopian Mustard (Brassica carinata A. Braun) Germplasm in Western Canada. Genetic Resources and Crop Evolution* 2006, *53(*2):297–312.

4.Hu J, Quiros CF: *APPLICATION OF MOLECULAR MARKERS AND CYTOGENETIC STOCKS TO BRASSICA GENETICS, BREEDING AND EVOLUTION. Acta Horticulturae* 1996(407):79–86.

5.U: *Genome analysis in Brassica with special reference to the experimental formation of B. napus and peculiar mode of fertilization. Journal of Japanese Bontany* 1935, *7.*

6.LUKENS LN, QUIJADA PA, UDALL J, PIRES JC, SCHRANZ ME, OSBORN TC: *Genome redundancy and plasticity within ancient and recent Brassica crop species. Biological Journal of the Linnean Society* 2004, *82(*4):665–674.

7.Song K, Osborn TC, Williams PH: *Brassica taxonomy based on nuclear restriction fragment length polymorphisms (RFLPs). Theoretical and Applied Genetics* 1990, *79(*4):497–506.

8.Alemayehu N, Becker H: *Genotypic diversity and patterns of variation in a germplasm material of Ethiopian mustard (Brassica carinata A. Braun). Genetic Resources and Crop Evolution* 2002, *49(*6):573–582.

9.Abebe D, Dawit T, Getahun M, Debritu B: *Ethiopia's genetic resources of oilseeds. In: Proc. 1 National Oilseeds Workshop. Institute of Agricultural Research, Addis Ababa, Ethiopia, pp 12–17* 1992.

10.Jiang Y, Tian E, Li R, Chen L, Meng J: *Genetic diversity of Brassica carinata with emphasis on the interspecific crossability with B. rapa. Plant Breeding* 2007, *126(*5):487–491.

11.Taylor DC, Falk KC, Palmer CD, Hammerlindl J, Babic V, Mietkiewska E, Jadhav A, Marillia E-F, Francis T, Hoffman T *et al: Brassica carinata—a new molecular farming platform for delivering bio-industrial oil feedstocks: case studies of genetic modifications to improve very long-chain fatty acid and oil content in seeds. Biofuels, Bioproducts and Biorefining* 2010, *4(*5):538–561.

12.Getinet A, Rakow G, Downey RK: *Agronomic performance and seed quality of Ethiopian mustard in Saskatchewan. Canadian Journal of Plant Science* 1996, *76(*3):387–392.

13.Meng J, Shi S, Gan L, Li Z, Qu X: *The production of yellow-seeded Brassica napus (AACC) through crossing interspecific hybrids of B. campestris (AA) and B. carinata (BBCC) with B. napus. Euphytica* 1998, *103(*3):329–333.

14.Tian E, Jiang Y, Chen L, Zou J, Liu F, Meng J: *Synthesis of a Brassica trigenomic allohexaploid (B. carinata × B. rapa) de novo and its stability in subsequent generations. Theoretical and Applied Genetics* 2010, *121(*8):1431–1440.

15.Xiao Y, Chen L, Zou J, Tian E, Xia W, Meng J: *Development of a population for substantial new type Brassica napus diversified at both A/C genomes. Theoretical and Applied Genetics* 2010, *121(*6):1141–1150.

16.Zou J, Zhu J, Huang S, Tian E, Xiao Y, Fu D, Tu J, Fu T, Meng J: *Broadening the avenue of intersubgenomic heterosis in oilseed Brassica. Theoretical and Applied Genetics* 2010, *120(*2):283–290.

17.Zou J, Hu D, Mason AS, Shen X, Wang X, Wang N, Grandke F, Wang M, Chang S, Snowdon RJ *et al: Genetic changes in a novel breeding population of Brassica napus synthesized from hundreds of crosses between B. rapa and B. carinata. Plant biotechnology journal* 2018, *16(*2):507–519.

18.Zou J, Raman H, Guo S, Hu D, Wei Z, Luo Z, Long Y, Shi W, Fu Z, Du D *et al: Constructing a dense genetic linkage map and mapping QTL for the traits of flower development in Brassica carinata. Theoretical and Applied Genetics* 2014, *127(7*):1593–1605.

19.Zhang W, Hu D, Raman R, Guo S, Wei Z, Shen X, Meng J, Raman H, Zou J: *Investigation of the Genetic Diversity and Quantitative Trait Loci Accounting for Important Agronomic and Seed Quality Traits in Brassica carinata.* In: *Frontiers in plant science.* vol. 8; 2017: 615.

20.Li D, Zhang X, Xu Y, Li L, Aghdam MS, Luo Z: *Effect of exogenous sucrose on anthocyanin synthesis in postharvest strawberry fruit. Food chemistry* 2019, *289:*112–120.

21.Pojer E, Mattivi F, Johnson D, Stockley CS: *The Case for Anthocyanin Consumption to Promote Human Health: A Review. Comprehensive Reviews in Food Science and Food Safety* 2013, *12(*5):483–508.

22.Prior RL, Xianli W: *Anthocyanins: structural characteristics that result in unique metabolic patterns and biological activities. Free Radic Res* 2006, *40(*10):1014–1028.

23.Mazza G, Miniati E: *Anthocyanins in fruits, vegetables, and grains. Anthocyanins in Fruits Vegetables & Grains* 1993.

24.Turturica M, Oancea A-M, Rapeanu G, Bahrim G: *Anthocyanins: Naturally occuring fruit pigments with functional properties. Annals of the University Dunarea de Jos of Galati Fascicle VI: Food Technology* 2015, *39:*9–24.

25.Khoo HE, Azlan A, Tang ST, Lim SM: *Anthocyanidins and anthocyanins: colored pigments as food, pharmaceutical ingredients, and the potential health benefits. Food & Nutrition Research* 2017, *61(*1):1361779.

26.Dong T, Han R, Yu J, Zhu M, Zhang Y, Gong Y, Li Z: *Anthocyanins accumulation and molecular analysis of correlated genes by metabolome and transcriptome in green and purple asparaguses (Asparagus officinalis, L.). Food chemistry* 2019, *271:*18–28.

27.Gamel TH, Wright AJ, Tucker AJ, Pickard M, Rabalski I, Podgorski M, Di Ilio N, O'Brien C, Abdel-Aal E-SM: *Absorption and metabolites of anthocyanins and phenolic acids after consumption of purple wheat crackers and bars by healthy adults. Journal of Cereal Science* 2019, *86:*60–68.

28.Sun D, Huang S, Cai S, Cao J, Han P: *Digestion property and synergistic effect on biological activity of purple rice (Oryza sativa L.) anthocyanins subjected to a simulated gastrointestinal digestion in vitro. Food research international* 2015, *78:*114–123.

29.Ferarsa S, Zhang W, Moulai-Mostefa N, Ding L, Jaffrin MY, Grimi N: *Recovery of anthocyanins and other phenolic compounds from purple eggplant peels and pulps using ultrasonic-assisted extraction. Food and Bioproducts Processing* 2018, *109:*19–28.

30.Lao F, Giusti MM: *Quantification of Purple Corn (Zea mays L.) Anthocyanins Using Spectrophotometric and HPLC Approaches: Method Comparison and Correlation. Food Analytical Methods* 2016, *9(*5):1367–1380.

31.Zhang H, Hassan YI, Renaud J, Liu R, Yang C, Sun Y, Tsao R: *Bioaccessibility, bioavailability, and anti-inflammatory effects of anthocyanins from purple root vegetables using mono- and co-culture cell models. Molecular nutrition & food research* 2017, *61(*10):1600928.

32.Szymanowska U, Złotek U, Karaś M, Baraniak B: *Anti-inflammatory and antioxidative activity of anthocyanins from purple basil leaves induced by selected abiotic elicitors. Food chemistry* 2015, *172:*71–77.

33.Lai Y-S, Li S, Tang Q, Li H-X, Chen S-X, Li P-W, Xu J-Y, Xu Y, Guo X: *The Dark-Purple Tea Cultivar 'Ziyan' Accumulates a Large Amount of Delphinidin-Related Anthocyanins. Journal of agricultural and food chemistry* 2016, *64(*13):2719–2726.

34.Ou L-j, Zhang Z-q, Dai X-z, Zou X-x: *Photooxidation Tolerance Characters of a New Purple Pepper. PloS one* 2013, *8(*5):e63593.

35.Yan C, An G, Zhu T, Zhang W, Zhang L, Peng L, Chen J, Kuang H: *Independent activation of the BoMYB2 gene leading to purple traits in Brassica oleracea. Theoretical and Applied Genetics* 2019, *132(*4):895–906.

36.Li H, Zhu L, Yuan G, Heng S, Yi B, Ma C, Shen J, Tu J, Fu T, Wen J: *Fine mapping and candidate gene analysis of an anthocyanin-rich gene, BnaA.PL1, conferring purple leaves in Brassica napus L. Molecular Genetics and Genomics* 2016, *291(*4):1523–1534.

37.Wang C, Li H, Li Y, Meng Q, Xie F, Xu Y, Wan Z: *Genetic characterization and fine mapping BrCER4 in involved cuticular wax formation in purple cai-tai (Brassica rapa L. var. purpurea). Molecular Breeding* 2019, *39(*1):12.

38.Zhao Z, Xiao L, Xu L, Xing X, Tang G, Du D: *Fine mapping the BjPl1 gene for purple leaf color in B2 of Brassica juncea L. through comparative mapping and whole-genome re-sequencing. Euphytica* 2017, *213(*4):80.

39.Wiese S, Reidegeld KA, Meyer HE, Warscheid B: *Protein labeling by iTRAQ: A new tool for quantitative mass spectrometry in proteome research. PROTEOMICS* 2007, *7(*3):340–350.

40.Wang W, Zhang D, Yu S, Liu J, Wang D, Zhang F, Yu Y, Zhao X, Lu G, Su T: *Mapping the BrPur gene for purple leaf color on linkage group A03 of Brassica rapa. Euphytica* 2014, *199(*3):293–302.

41.Cheng GW, Breen PJ: *Activity of Phenylalanine Ammonia-Lyase (PAL) and Concentrations of Anthocyanins and Phenolics in Developing Strawberry Fruit. Journal of the American Society for Horticultural Science* 1991, *116(*5).

42.Wang J, Zhang H, Zhang J, Zhang H, Liu B, Hou Y, Qiu N: *Changes of Anthocyanin Content and Photosynthetic Function of Purple Leaf Plum Leaves during Spring Maturation. FORESTRY SCIENCE & TECHNOLOGY* 2018, *43(*03):13–17.

43.Yu X: *Analysis and Study of Anthocyanins in Plant Leave Modern Instruments* 2000(04):37–38.

44.Yonekura-Sakakibara K, Fukushima A, Nakabayashi R, Hanada K, Matsuda F, Sugawara S, Inoue E, Kuromori T, Ito T, Shinozaki K *et al: Two glycosyltransferases involved in anthocyanin modification delineated by transcriptome independent component analysis in Arabidopsis thaliana. The Plant Journal* 2012, *69(*1):154–167.

45.Luo J, Nishiyama Y, Fuell C, Taguchi G, Elliott K, Hill L, Tanaka Y, Kitayama M, Yamazaki M, Bailey P *et al: Convergent evolution in the BAHD family of acyl transferases: identification and characterization of anthocyanin acyl transferases from Arabidopsis thaliana. The Plant Journal* 2007, *50(*4):678–695.

46.Miyahara T, Sakiyama R, Ozeki Y, Sasaki N: *Acyl-glucose-dependent glucosyltransferase catalyzes the final step of anthocyanin formation in Arabidopsis. Journal of Plant Physiology* 2013, *170(*6):619–624.

47.Tohge T, Nishiyama Y, Hirai MY, Yano M, Nakajima J-i, Awazuhara M, Inoue E, Takahashi H, Goodenowe DB, Kitayama M *et al: Functional genomics by integrated analysis of metabolome and transcriptome of Arabidopsis plants over-expressing an MYB transcription factor. The Plant Journal* 2005, *42(*2):218–235.

48.Bowles D: *A multigene family of glycosyltransferases in a model plant, Arabidopsis thaliana. Biochemical Society Transactions* 2002, *30(*2):301–306.

49.Guo Y, Chang X, Zhu C, Zhang S, Li X, Fu H, Chen C, Lin Y, Lai Z: *De novo transcriptome combined with spectrophotometry and gas chromatography-mass spectrometer (GC-MS) reveals differentially expressed genes during accumulation of secondary metabolites in purple-leaf tea (Camellia sinensis cv Hongyafoshou). The Journal of Horticultural Science and Biotechnology* 2019, *94(*3):349–367.

50.Chen D, Liu Y, Pan Q, Li F, Zhang Q, Ge X, Li Z: *De novo transcriptome assembly, gene expressions and metabolites for flower color variation of two garden species in Brassicaceae. Scientia Horticulturae* 2018, *240:*592–602.

51.Ziegler H: *Nature of Transported Substances.* In: *Transport in Plants I: Phloem Transport.* Edited by Zimmermann MH, Milburn JA. Berlin, Heidelberg: Springer Berlin Heidelberg; 1975: 59–100.

52.Chiou T-J, Bush DR: *Sucrose is a signal molecule in assimilate partitioning. Proceedings of the National Academy of Sciences* 1998, *95(*8):4784–4788.

53.Solfanelli C, Poggi A, Loreti E, Alpi A, Perata P: *Sucrose-Specific Induction of the Anthocyanin Biosynthetic Pathway in Arabidopsis. Plant physiology* 2006, *140(*2):637–646.

54.Ai TN, Naing AH, Arun M, Lim S-H, Kim CK: *Sucrose-induced anthocyanin accumulation in vegetative tissue of Petunia plants requires anthocyanin regulatory transcription factors. Plant Science* 2016, *252:*144–150.

55.Kim SH, Kim Y-S, Jo YD, Kang S-Y, Ahn J-W, Kang B-C, Kim J-B: *Sucrose and methyl jasmonate modulate the expression of anthocyanin biosynthesis genes and increase the frequency of flower-color*

mutants in chrysanthemum. Scientia Horticulturae 2019, *256:*108602.

56.Wang S, Pan D, Lv X, Song X, Qiu Z, Huang C, Huang R, Chen W: *Proteomic approach reveals that starch degradation contributes to anthocyanin accumulation in tuberous root of purple sweet potato. Journal of proteomics* 2016, *143:*298–305.

57.Tan H, Man C, Xie Y, Yan J, Chu J, Huang J: *A Crucial Role of GA-Regulated Flavonol Biosynthesis in Root Growth of Arabidopsis. Molecular plant* 2019, *12(*4):521–537.

58.Karppinen K, Tegelberg P, Häggman H, Jaakola L: *Abscisic Acid Regulates Anthocyanin Biosynthesis and Gene Expression Associated With Cell Wall Modification in Ripening Bilberry (Vaccinium myrtillus L.) Fruits. Frontiers in plant science* 2018, *9(*1259).

59.Sun Y, Liu Q, Xi B, Dai H: *Study on the regulation of anthocyanin biosynthesis by exogenous abscisic acid in grapevine. Scientia Horticulturae* 2019, *250:*294–301.

60.Kim D, Bahmani R, Ko J-H, Hwang S: *Development of bisphenol A (BPA)-sensing indicator Arabidopsis thaliana which synthesizes anthocyanin in response to BPA in leaves. Ecotoxicology and Environmental Safety* 2019, *170:*627–634.

61.Kumar D, Sarmah BK, Das PK: *Ethylene mediates repression of anthocyanin accumulation in black rice pericarps in the absence of light. Journal of Plant Physiology* 2019, *236:*34–38.

62.Li Y, Li H, Wang F, Li J, Zhang Y, Wang L, Gao J: *Comparative Transcriptome Analysis Reveals Effects of Exogenous Hematin on Anthocyanin Biosynthesis during Strawberry Fruit Ripening. International Journal of Genomics* 2016, *2016:*14.

63.Jezek M, Zörb C, Merkt N, Geilfus CM: *Anthocyanin management in fruits by fertilization. Journal of Agricultural & Food Chemistry* 2018, *66(*4):acs.jafc.7b03813.

64.Luo J, Wang X, Feng L, Li Y, He J-X: *The mitogen-activated protein kinase kinase 9 (MKK9) modulates nitrogen acquisition and anthocyanin accumulation under nitrogen-limiting condition in Arabidopsis. Biochemical and biophysical research communications* 2017, *487(*3):539–544.

65.Truong HA, Lee WJ, Jeong CY, Trịnh CS, Lee S, Kang C-S, Cheong Y-K, Hong S-W, Lee H: *Enhanced anthocyanin accumulation confers increased growth performance in plants under low nitrate and high salt stress conditions owing to active modulation of nitrate metabolism. Journal of Plant Physiology* 2018, *231:*41–48.

66.Wang ZQ, Zhou X, Dong L, Guo J, Chen Y, Zhang Y, Wu L, Xu M: *iTRAQ-based analysis of the Arabidopsis proteome reveals insights into the potential mechanisms of anthocyanin accumulation regulation in response to phosphate deficiency. Journal of proteomics* 2018, *184:*39–53.

67.Zhang KM, Guo ML, He D, Wu RH, Li YH: *The Inhibition Effect and Excessive Carbon Flux Resulting from Blocking Anthocyanin Biosynthesis Under Darkness in Begonia semperflorens. Journal of Plant Growth Regulation* 2016, *35(*1):22–30.

68.Zhang H-N, Li W-C, Wang H-C, Shi S-Y, Shu B, Liu L-Q, Wei Y-Z, Xie J-H: *Transcriptome Profiling of Light-Regulated Anthocyanin Biosynthesis in the Pericarp of Litchi. Frontiers in plant science* 2016, *7(*963).

69.Li J, Ren L, Gao Z, Jiang M, Liu Y, Zhou L, He Y, Chen H: *Combined transcriptomic and proteomic analysis constructs a new model for light-induced anthocyanin biosynthesis in eggplant (Solanum melongena L.). Plant, cell & environment* 2017, *40(*12):3069–3087.

70.Xu P, Zawora C, Li Y, Wu J, Liu L, Liu Z, Cai R, Lian H: *Transcriptome sequencing reveals role of light in promoting anthocyanin accumulation of strawberry fruit. Plant Growth Regulation* 2018, *86(*1):121–132.

71.Zhang KM, Wang JW, Guo ML, Du WL, Wu RH, Wang X: *Short-day signals are crucial for the induction of anthocyanin biosynthesis in Begonia semperflorens under low temperature condition. Journal of Plant Physiology* 2016, *204:*1–7.

72.Bhatia C, Pandey A, Gaddam SR, Hoecker U, Trivedi PK: *Low Temperature-Enhanced Flavonol Synthesis Requires Light-Associated Regulatory Components in Arabidopsis thaliana. Plant and Cell Physiology* 2018, *59(*10):2099–2112.

73.Zhu Z, Wang H, Wang Y, Guan S, Wang F, Tang J, Zhang R, Xie L, Lu Y: *Characterization of the cis elements in the proximal promoter regions of the anthocyanin pathway genes reveals a common regulatory logic that governs pathway regulation. Journal of experimental botany* 2015, *66(*13):3775–3789.

74.Gonzalez A, Zhao M, Leavitt JM, Lloyd AM: *Regulation of the anthocyanin biosynthetic pathway by the TTG1/bHLH/Myb transcriptional complex in Arabidopsis seedlings. The Plant Journal* 2008, *53(*5):814–827.

75.Zhang Y, Chu G, Hu Z, Gao Q, Cui B, Tian S, Wang B, Chen G: *Genetically engineered anthocyanin pathway for high health-promoting pigment production in eggplant. Molecular Breeding* 2016, *36(*5):54.

Table 1

Table 1 Relative differences in the expression levels of the proteins involved in the anthocyanin biosynthesis pathway between purple-leaved and green-leaved Ethiopian mustard.

Serial number	Protein ID	Description	Gene name	Fold change（BC-P01 versus BC-G02）	P-value
1	TRINITY_DN5961_c0_g2	anthocyanin 5-O-glucosyltransferase	UGT75C1	2.13	0.000
2	TRINITY_DN5961_c0_g1		UGT75C1	2.07	0.001
3	TRINITY_DN8427_c0_g1	anthocyanin 2''-O-xylosyltransferase	UGT79B1	2.32	0.007

Figures

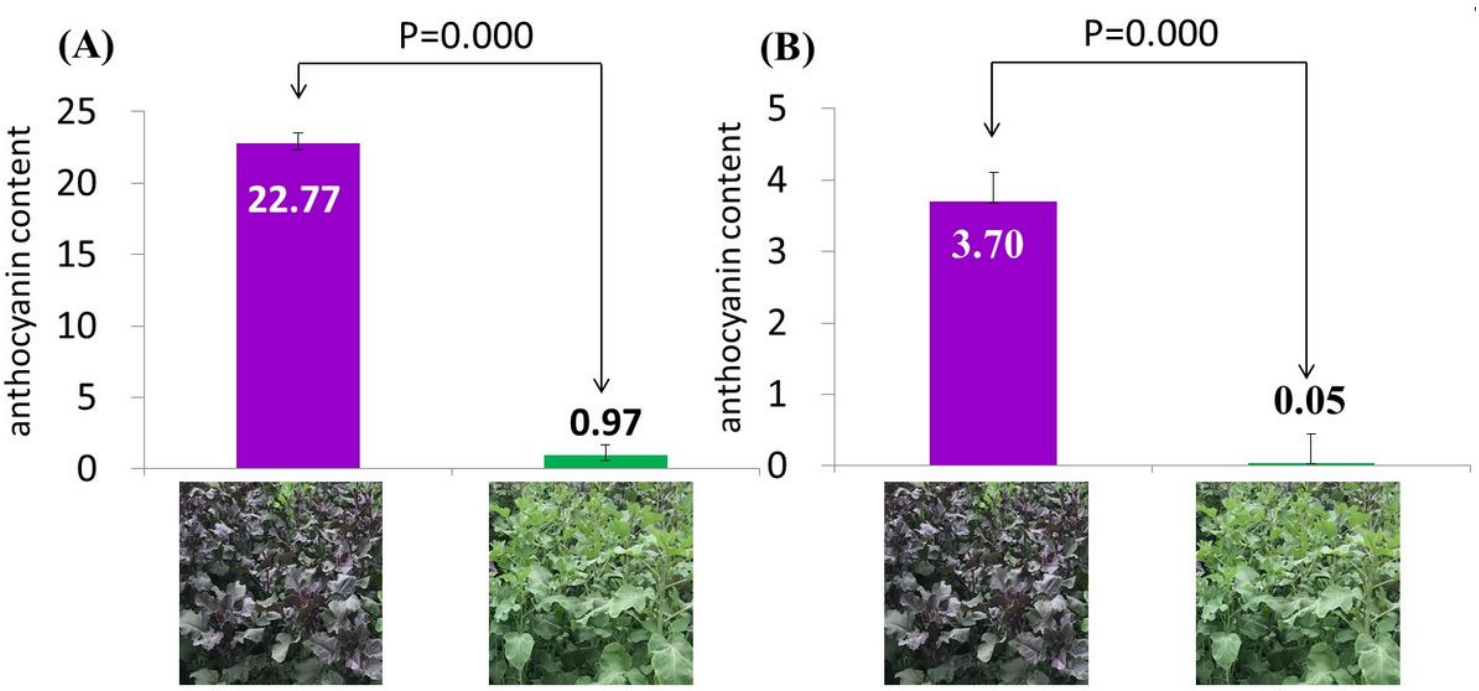

Figure 1

The total anthocyanin content determined by the simplified method (A, g·10 mL 0.1 mol/L hydrochloric acid) and pH differential method (B, mg·g-1) in Ethiopian mustard (B. carinata) lines with purple and green leaves.

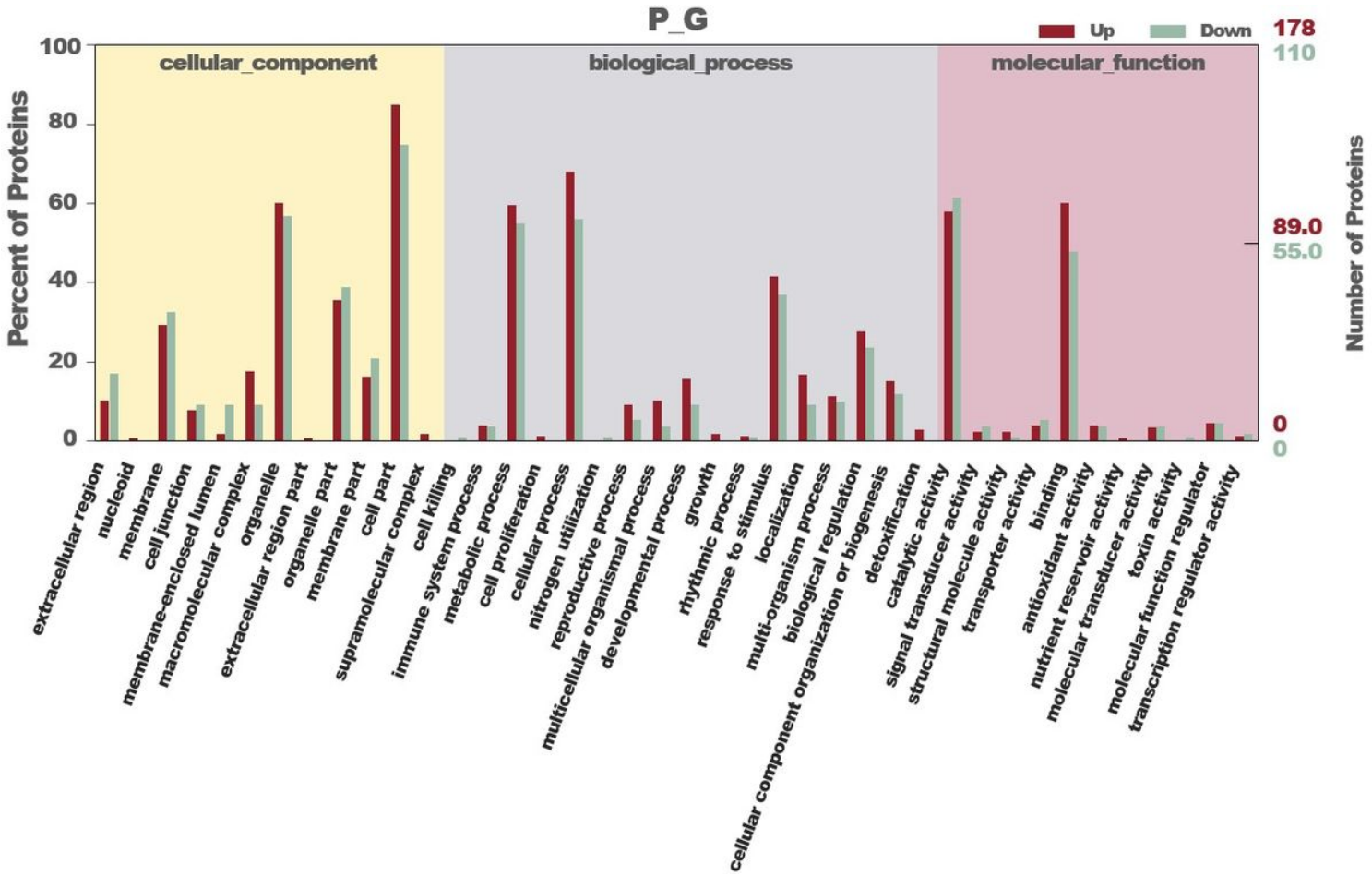

Figure 2

Gene Ontology (GO) functional annotation analysis of the DEPs, covering a wide range of biological processes, cellular components and molecular functions.

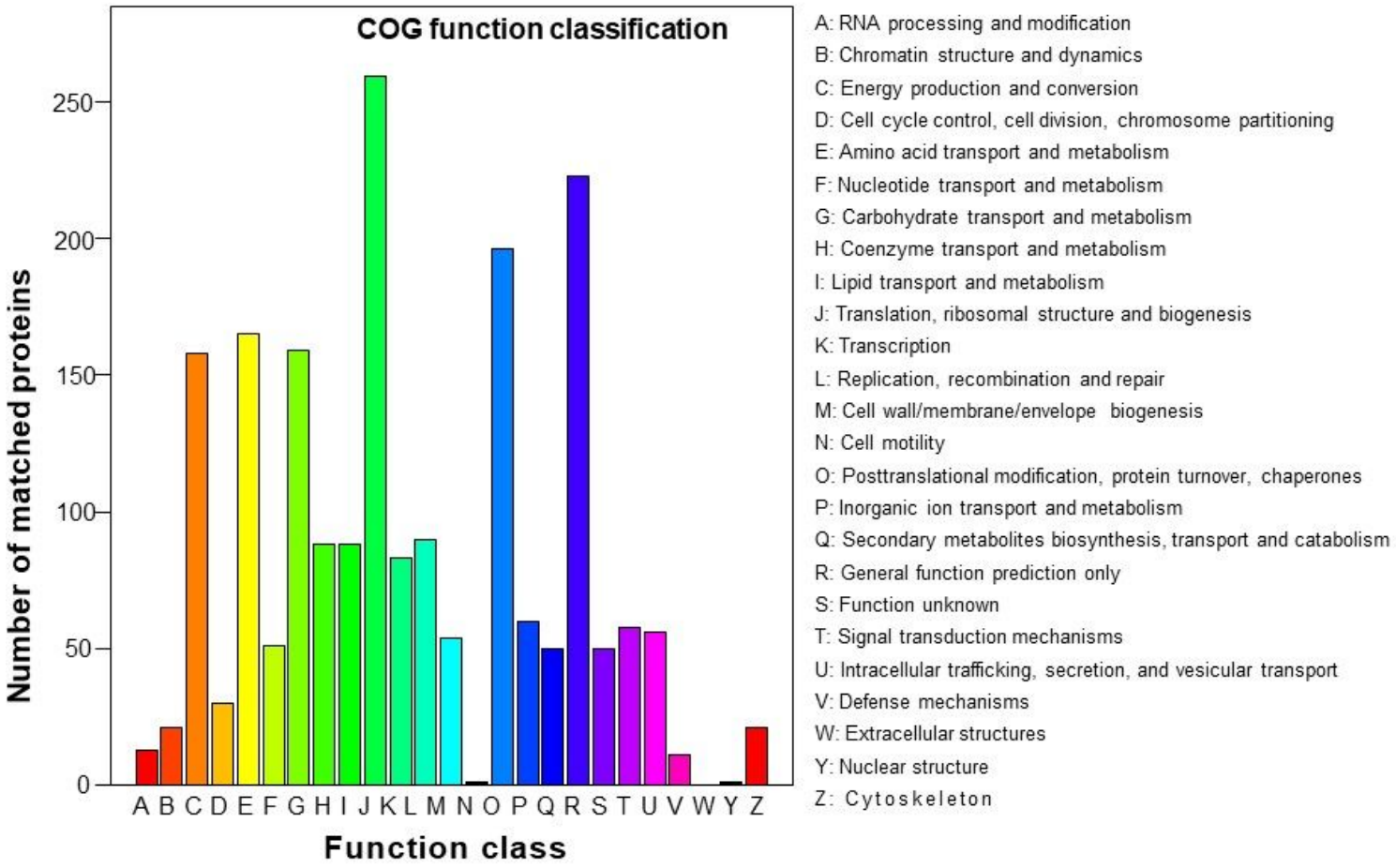

Figure 3

COG annotation of the DEPs, which are divided into 25 categories.

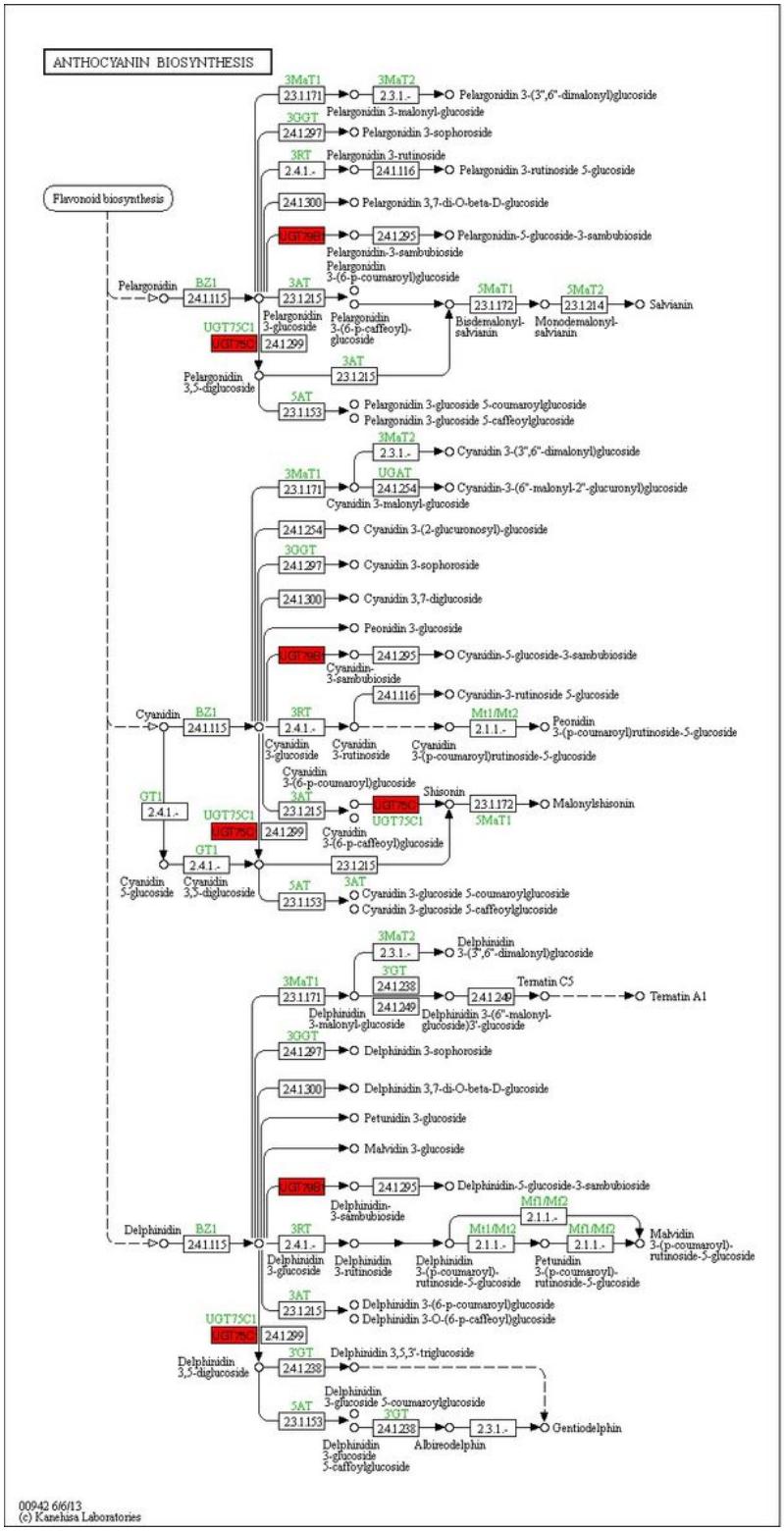

Figure 4

The anthocyanin metabolic pathway, including three upregulated proteins identified in this study.

Supplementary Files

This is a list of supplementary files associated with this preprint. Click to download.

- SupplementaryTable1DEPs.xlsx
- SupplementaryTable5KEGG.xlsx
- SupplementaryFig.1.docx
- SupplementaryTable2TF.xls
- SupplementaryTable4COG.xlsx
- SupplementaryFig.2Hierarchicalclustering.docx
- SupplementaryTable3GO.xlsx